Superconductivity at the brink of spin/charge order

Oskar Vafek

June 14, 2016

Contents

1 Motivation and the non-interacting model

This lecture is about a class of realistic models on the A-B stacked honeycomb bilayer with purely repulsive interactions, which at half filling develop either a spin order, such as antiferromagnetism, or a charge order, such as a nematic. When doped, we find Cooper pairing and the ground state is a superconductor. Upon further doping, superconductivity disappears. These models are sufficiently tractable that the mechanism of pairing can be clearly identified. Moreover, it provides an explicit example of the notion of intertwined orders, mentioned by Steve Kivelson in his Boulder 2014 lectures.

If we consider hopping of electrons on the A-B stacked honeycomb bilayer, shown in the Figure (1), we find four bands, because there are four atoms per unit cell. Two bands touch at $\mathbf{K} = \frac{4\pi}{3\sqrt{3}}\hat{y}$ and $-\mathbf{K}$ points in the Brilloin zone shown here. If we take into account only the nearest neighbor hopping, in the graphene field denoted by γ_0 and γ_1, we find that two of the four bands are split off by the interlayer tuneling γ_1, and the remaining two touch parabolicaly.

Explicitly, taking the lattice spacing $a = 1$,

$$\begin{aligned}
\mathcal{H}_0 &= \sum_{\mathbf{r}}\sum_{j=1}^{3}\gamma_0\left(c^\dagger_{A_1,\mathbf{r}}c_{B_1,\mathbf{r}+\delta_j} + c^\dagger_{A_2,\mathbf{r}}c_{B_2,\mathbf{r}-\delta_j} + H.c.\right) && (1)\\
&+ \sum_{\mathbf{r}}\left(\gamma_1 c^\dagger_{A_1,\mathbf{r}}c_{A_2,\mathbf{r}} + H.c.\right). && (2)\\
&= \sum_{\mathbf{k}}\left(D_{\mathbf{k}}c^\dagger_{A_1}(\mathbf{k})c_{B_1}(\mathbf{k}) + D^*_{\mathbf{k}}c^\dagger_{A_2}(\mathbf{k})c_{B_2}(\mathbf{k}) + \gamma_1 c^\dagger_{A_1}(\mathbf{k})c_{A_2}(\mathbf{k}) + H.c.\right) && (3)\\
&= \sum_{\mathbf{k}}\left(c^\dagger_{B_1}(\mathbf{k}), c^\dagger_{B_2}(\mathbf{k}), c^\dagger_{A_1}(\mathbf{k}), c^\dagger_{A_2}(\mathbf{k})\right)\begin{pmatrix} 0 & 0 & D^*_{\mathbf{k}} & 0\\ 0 & 0 & 0 & D_{\mathbf{k}}\\ D_{\mathbf{k}} & 0 & 0 & \gamma_1\\ 0 & D^*_{\mathbf{k}} & \gamma_1 & 0\end{pmatrix}\begin{pmatrix} c_{B_1}(\mathbf{k})\\ c_{B_2}(\mathbf{k})\\ c_{A_1}(\mathbf{k})\\ c_{A_2}(\mathbf{k})\end{pmatrix} && (4)
\end{aligned}$$

where $\delta_1 = \hat{x}$, $\delta_2 = -\frac{\hat{x}}{2} + \frac{\sqrt{3}}{2}\hat{y}$, and $\delta_2 = -\frac{\hat{x}}{2} - \frac{\sqrt{3}}{2}\hat{y}$.

$$D_{\mathbf{k}} = \gamma_0\left(e^{ik_x} + 2e^{-\frac{i}{2}k_x}\cos\left(\frac{\sqrt{3}}{2}k_y\right)\right). \quad (5)$$

Note that at $\pm\mathbf{K} = \pm\frac{4\pi}{3\sqrt{3}}\hat{y}$, we have $D_{\pm\mathbf{K}} = 0$, and

$$D_{\pm\mathbf{K}+\mathbf{k}} = \gamma_0 a\frac{3i}{2}\left(k_x \pm ik_y\right) + \mathcal{O}(k^2).$$

Clearly, at $\pm\mathbf{K}$, we have a doublet at zero energy, and two states which are split-off to $\pm\gamma_1$.

Now, formulate this problem as a coherent state Grassmann path-integral:

$$\begin{aligned}
Z_0 &= \int \mathcal{D}(\psi^*_A, \psi_A, \psi^*_B, \psi_B)e^{-S_0} && (6)\\
S_0 &= \sum_n\sum_{\mathbf{k}}\left(\psi^*_A\left(-i\omega_n 1 + \gamma_1\sigma_1\right)\psi_A - i\omega_n\psi^*_B\psi_B + \psi^*_B\begin{pmatrix} D^*_{\mathbf{k}} & 0\\ 0 & D_{\mathbf{k}}\end{pmatrix}\psi_A + \psi^*_A\begin{pmatrix} D_{\mathbf{k}} & 0\\ 0 & D^*_{\mathbf{k}}\end{pmatrix}\psi_B\right) && (7)
\end{aligned}$$

Now, integrate out the (high energy) ψ_A-modes. The resulting effective action for the ψ_B-modes is

$$\begin{aligned}
Z_0 &= const.\times\int\mathcal{D}(\psi^*_B, \psi_B)e^{-S_{eff}} && (8)\\
S^{(0)}_{eff} &= \sum_n\sum_{\mathbf{k}}\left[-i\omega_n\psi^*_B\psi_B - \psi^*_B\begin{pmatrix} D^*_{\mathbf{k}} & 0\\ 0 & D_{\mathbf{k}}\end{pmatrix}\left(-i\omega_n 1 + \gamma_1\sigma_1\right)^{-1}\begin{pmatrix} D_{\mathbf{k}} & 0\\ 0 & D^*_{\mathbf{k}}\end{pmatrix}\psi_B\right] && (9)
\end{aligned}$$

Now,

$$\begin{pmatrix} D^*_{\mathbf{k}} & 0\\ 0 & D_{\mathbf{k}}\end{pmatrix}\left(-i\omega_n 1 + \gamma_1\sigma_1\right)^{-1}\begin{pmatrix} D_{\mathbf{k}} & 0\\ 0 & D^*_{\mathbf{k}}\end{pmatrix} = \frac{1}{\omega_n^2 + \gamma_1^2}\begin{pmatrix} i\omega_n D^*_{\mathbf{k}}D_{\mathbf{k}} & \gamma_0 {D^*_{\mathbf{k}}}^2\\ \gamma_0 {D_{\mathbf{k}}}^2 & i\omega_n D_{\mathbf{k}}D^*_{\mathbf{k}}\end{pmatrix}. \quad (10)$$

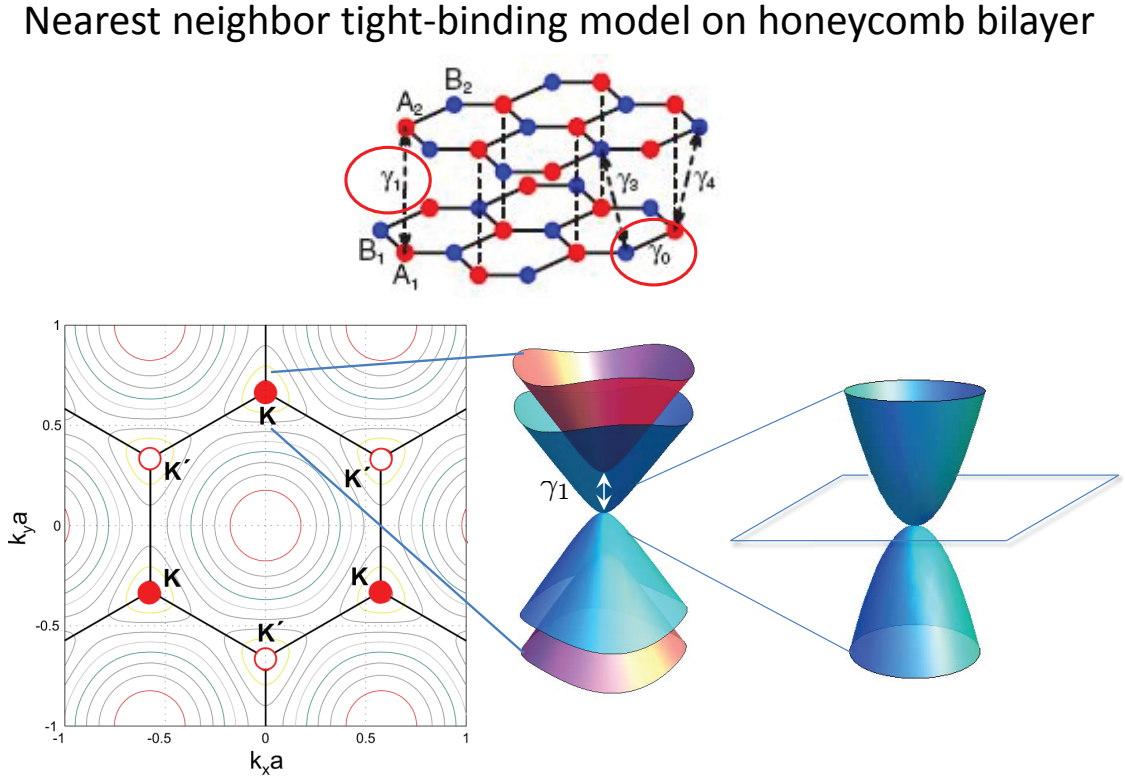

Figure 1: Schematic of the A-B stacked honeycomb bilayer and the resulting dispersion.

We are interested in energies much smaller than γ_0, the energy of the split-off bands. The terms on the diagonal are $\sim \omega_n \mathbf{k}^2$ and the terms on the off-diagonal have one power of ω_n less. Therefore, in the low energy regime, we can ignore the diagonal term which we have generated, and focus only on the off-diagonal term. Therefore, defining a four-component field by expanding near $\pm\mathbf{K}$:

$$\psi_{n,\mathbf{k}} = \begin{pmatrix} c_{B_1}(\omega_n, \mathbf{K}+\mathbf{k}) \\ c_{B_2}(\omega_n, \mathbf{K}+\mathbf{k}) \\ c_{B_1}(\omega_n, -\mathbf{K}+\mathbf{k}) \\ c_{B_2}(\omega_n, -\mathbf{K}+\mathbf{k}) \end{pmatrix}. \tag{11}$$

we find (adding the electron spin):

$$\begin{aligned} S^{(0)}_{eff} &\approx \sum_n \sum_{|\mathbf{k}|<\Lambda} \sum_{\sigma=\uparrow,\downarrow} \left[-i\omega_n \psi^\dagger_{n,\mathbf{k},\sigma}\psi_{n,\mathbf{k},\sigma} + \psi^\dagger_{n,\mathbf{k},\sigma} \left(\frac{k_x^2 - k_y^2}{2m^*} 1\sigma_1 + \frac{k_x k_y}{m^*}\tau_3\sigma_2 \right) \psi_{n,\mathbf{k},\sigma} \right] \\ &= \int_0^\beta d\tau \int d^2\mathbf{r} \sum_{\sigma=\uparrow,\downarrow} \left[\psi^\dagger_\sigma(\mathbf{r},\tau)\frac{\partial}{\partial\tau}\psi_\sigma(\mathbf{r},\tau) + \psi^\dagger_\sigma(\mathbf{r},\tau) \left(\frac{p_x^2 - p_y^2}{2m^*} 1\sigma_1 + \frac{p_x p_y}{m^*}\tau_3\sigma_2 \right) \psi_\sigma(\mathbf{r},\tau) \right] \end{aligned} \tag{12}$$

where $\beta = \frac{1}{k_B T}$. Note that at $T = 0$, $S^{(0)}_{eff}$ is invariant upon the following scaling transformation

$$\mathbf{r} = s\mathbf{r}' \tag{13}$$

$$\tau = s^2\tau' \tag{14}$$

$$\psi_\sigma(s\mathbf{r}', s^2\tau') = \frac{1}{s}\psi'_\sigma(\mathbf{r}', \tau'). \tag{15}$$

At finite T, we can make it invariant by including the rescaling of temperature $T' = s^2 T$.

Under the Wilsonian renormalization group procedure, we eliminate all modes $\psi_{n,\mathbf{k},\sigma}$ within a thin shell $(1-d\ell)\Lambda < |\mathbf{k}| < \Lambda$, but for all n and σ. Upon rescaling (13), the cutoff is send back to Λ. Clearly, $S^{(0)}_{eff}$ is left unchanged under this procedure. We can therefore think of $S^{(0)}_{eff}$ as a Gaussian fixed point with dynamical critical exponent $z = 2$.

2 Electron-electron interactions and the RG flow equations

Electron-electron interactions are represented by quartic terms in ψ in the action. If we start with finite range interactions at the microscopic lattice level, then we will generate local terms only. Note that upon rescling (13), the only local quartic terms which do not decrease under the RG procedure are of the form

$$S^{int}_{eff} = \frac{1}{2}\sum_{M,N}\int d\tau \int d^2\mathbf{r} G_{M,N}\left(\psi^\dagger_\sigma(\mathbf{r},\tau) M \psi_\sigma(\mathbf{r},\tau)\right)\left(\psi^\dagger_{\sigma'}(\mathbf{r},\tau) N \psi_{\sigma'}(\mathbf{r},\tau)\right), \tag{16}$$

where M and N are some 4×4 matrices. Quartic terms with derivatives or terms with more than 4 ψ terms scale down under the RG transformation.

Because there are 16-independent 4×4 matrices, naively, there are $2\times(16\times 15/2+16) = 272$ terms which we can write down for S^{int}_{eff}, corresponding to a large number of independent couplings $G_{M,N}$. However, time reversal symmetry, spin SU(2) symmetry, and the space group symmetry and Fierz identities relating spin singlet contact terms and spin triplet contact terms, reduce the total number of independent couplings to 9 (see OV PRB 82, 205106 (2010)). They are:

$$S^{int}_{eff} = \frac{2\pi}{m^*}\sum_{j=1}^{9} g_j \sum_{m=1}^{m_j}\int d\tau \int d^2\mathbf{r}\left(\psi^\dagger_\sigma(\mathbf{r},\tau)\Gamma^{(m)}_j \psi_\sigma(\mathbf{r},\tau)\right)\left(\psi^\dagger_{\sigma'}(\mathbf{r},\tau)\Gamma^{(m)}_j \psi_{\sigma'}(\mathbf{r},\tau)\right). \tag{17}$$

where the factor involving m^* was introduced to make g dimensionless, m_j is the multiplicity of the representation j, and where

$$A_{1g} : \Gamma^{(1)}_1 = 1_4 \tag{18}$$
$$A_{2g} : \Gamma^{(1)}_2 = \tau_3\sigma_3 \tag{19}$$
$$E_g : \Gamma^{(1)}_3 = 1\sigma_1, \Gamma^{(2)}_3 = \tau_3\sigma_2 \tag{20}$$
$$A_{1u} : \Gamma^{(1)}_4 = \tau_3 1 \tag{21}$$
$$A_{2u} : \Gamma^{(1)}_5 = 1\sigma_3 \tag{22}$$
$$E_u : \Gamma^{(1)}_6 = \tau_3\sigma_1, \Gamma^{(2)}_6 = -1\sigma_2 \tag{23}$$
$$A_{\mathbf{K}} : \Gamma^{(1)}_7 = \tau_1\sigma_1, \Gamma^{(2)}_7 = \tau_2\sigma_1 \tag{24}$$
$$A_{\mathbf{K}} : \Gamma^{(1)}_8 = \tau_1\sigma_2, \Gamma^{(2)}_8 = \tau_2\sigma_2 \tag{25}$$
$$E_{\mathbf{K}} : \Gamma^{(1)}_9 = \tau_1 1, \Gamma^{(2)}_9 = -\tau_2\sigma_3, \Gamma^{(3)}_9 = -\tau_2 1, \Gamma^{(4)}_9 = -\tau_1\sigma_3. \tag{26}$$

2.1 Details of the RG derivation

For general coupling constants g_{ST}, expanding in powers of g, gives cumulant expansion

$$\langle e^{-\frac{1}{2}g_{ST}\int_1 \psi^\dagger S\psi\psi^\dagger T\psi(1)}\rangle \approx e^{-\frac{1}{2}g_{ST}\left\langle\int_1 \psi^\dagger S\psi\psi^\dagger T\psi(1)\right\rangle}$$
$$\times\ \exp\left[\frac{g_{ST}g_{UV}}{8}\int_{1,2}\left(\left\langle\left(\psi^\dagger S\psi\psi^\dagger T\psi(1)\right)\left(\psi^\dagger U\psi\psi^\dagger V\psi(2)\right)\right\rangle - \left\langle\left(\psi^\dagger S\psi\psi^\dagger T\psi(1)\right)\right\rangle\left\langle\left(\psi^\dagger U\psi\psi^\dagger V\psi(2)\right)\right\rangle\right)\right]$$

where the average $\langle\ldots\rangle$ is with respect to the gaussian weighting factor. We have used a short-hand $1,2$ for the modes at space-(imaginary)time $\tau_{1,2}, \mathbf{r}_{1,2}$ and each $\psi = \psi_> + \psi_<$. We integrate over the fast modes $\psi_>$

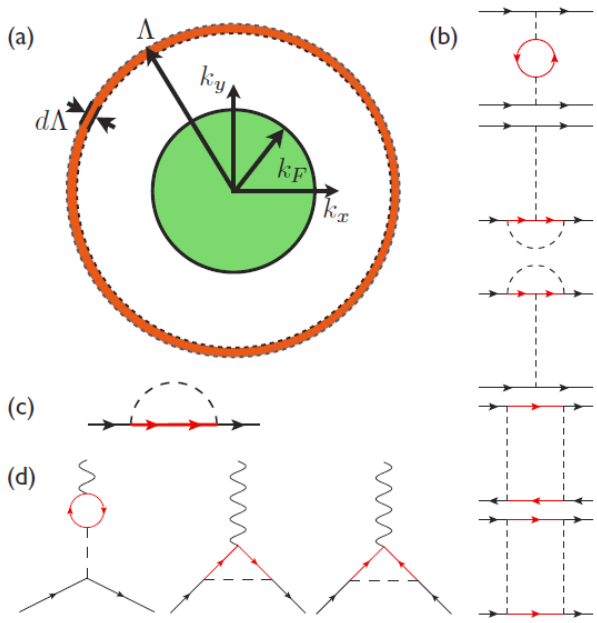

Figure 2: Schematic representation of the RG procedure. (a) We eliminate all modes $\psi_{n,\mathbf{k},\sigma}$ within a thin shell $(1-d\ell)\Lambda < |\mathbf{k}| < \Lambda$, but for all n and σ. (b) Diagrams contributing to the flow of the couplings. (c) Diagrams contributing to the determination of susceptibilities. From: J. Murray and OV, PRB 89, 205119 (2014)

whose wavenumbers $\Lambda/s < |\mathbf{k}| < \Lambda$. The non-interacting Green's function is

$$G_{\mathbf{k}}(\omega) = (-i\omega + \Sigma \cdot d_{\mathbf{k}})^{-1} = \frac{i\omega + \Sigma \cdot d_{\mathbf{k}}}{\omega^2 + \left(\frac{\mathbf{k}^2}{2m}\right)^2} \tag{27}$$

and $d^x_{\mathbf{k}} = \frac{k_x^2 - k_y^2}{2m^*}$, $d^y_{\mathbf{k}} = \frac{2k_x k_y}{2m^*}$, and $\Sigma^x = 1_4\sigma_1$, $\Sigma^y = 1\tau_3\sigma_2$.

Using the identity,

$$\int_{-\infty}^{\infty}\frac{d\omega}{2\pi}\int_{(1-d\ell)\Lambda}^{\Lambda}\frac{dkk}{2\pi}\int_0^{2\pi}\frac{d\theta}{2\pi}G_{\mathbf{k}}(\omega)\otimes G_{\mp\mathbf{k}}(\mp\omega) = \left(\pm 1_8\otimes 1_8 + \frac{1}{2}\Sigma^x\otimes\Sigma^x + \frac{1}{2}\Sigma^y\otimes\Sigma^y\right)\frac{m^*}{4\pi}d\ell, \tag{28}$$

we can evaluate the needed diagrams. All possible contractions correspond to the diagrams in the Figure (2b).

For the first diagram we find the following terms

$$\Delta S^{(RPA)}_{eff} = \frac{1}{2}\sum_S\sum_U g_S g_U\int_1\int_2\psi^\dagger(1)S\psi(1)\mathrm{Tr}\left[SG(1-2)UG(2-1)\right]\psi^\dagger(2)U\psi(2). \tag{29}$$

Using the gradient expansion to determine the RG fate of the marginal couplings and find

$$\Delta S^{(RPA)}_{eff} = \frac{1}{2}\sum_S\sum_U g_S g_U\int_1\psi^\dagger(1)S\psi(1)\mathrm{Tr}\left[-SU + \frac{1}{2}S\Sigma^xU\Sigma^x + \frac{1}{2}S\Sigma^yU\Sigma^y\right]\psi^\dagger(1)U\psi(1)\frac{m}{4\pi}d\ell. \tag{30}$$

For the second and third (vertex) diagrams in the Figure (2b) we have the following terms

$$\Delta S^{(V)}_{eff} = -\sum_S\sum_U g_S g_U\int_1\int_2\psi^\dagger(1)SG(1-2)UG(2-1)S\psi(1)\psi^\dagger(2)U\psi(2). \tag{31}$$

Performing the gradient expansion gives

$$\Delta S_{eff}^{(V)} = -\sum_S \sum_U g_S g_U \int_1 \psi^\dagger(1) S \left(-U + \frac{1}{2}\Sigma^x U \Sigma^x + \frac{1}{2}\Sigma^y U \Sigma^y \right) S\psi(1)\psi^\dagger(1) U \psi(1) \frac{m}{4\pi} d\ell. \quad (32)$$

For the fourth and the fifth diagrams in the Figure (2b) we find the following terms

$$\Delta S_{eff}^{(L)} = -\frac{1}{4}\sum_{S,U} g_S g_U \int_1 \left(\left(\psi^\dagger(1)\left[S,U\right]\psi(1)\right)^2 + \frac{1}{2}\sum_{a=x,y}\left(\psi^\dagger(1)\left(S\Sigma^a U + U\Sigma^a S\right)\psi(1)\right)^2 \right) \frac{m}{4\pi} d\ell. \quad (33)$$

2.2 RG equations

Adding the terms from $\Delta S_{eff}^{(RPA)}$, $\Delta S_{eff}^{(V)}$, and $\Delta S_{eff}^{(L)}$, from the previous subsection, rescaling the fields and the integration measure, and comparing to the starting action) we find the RG equations for the nine coupling constants:

$$\frac{dg_i}{d\ell} = A_{ijk} g_j g_k \quad (34)$$

where A_{ijk} are numbers. The each of the first order non-linear differential equations in (34) is left invariant upon

$$g_j \to b g_j \quad (35)$$
$$\ell \to \ell / b. \quad (36)$$

Therefore, any solution to Eq.(34) has the form

$$g_i(\ell, \{g_j(0)\}) = g \times \Phi_i \left(g\ell, \left\{ \frac{g_j(0)}{g} \right\} \right), \quad (37)$$

$$g = \sqrt{\sum_{j=1}^{9} g_j^2(0)}, \quad (38)$$

where $\Phi_i's$ are functions which can be determined numerically. They typically diverge at some ℓ_*.

In the special case of initially having only forward scattering interaction $g_{A_{1g}}$, i.e. only $\left(\psi_\sigma^\dagger 1 \psi_\sigma\right)^2$, the flow equations simplify to

$$\frac{dg_{A1g}}{d\ell} = -4 g_{A1g} g_{Eg}, \quad (39)$$
$$\frac{dg_{A2g}}{d\ell} = -12 g_{A2g}^2 + 4 g_{Eg}^2 + 4 g_{A1g} g_{A2g} - 12 g_{A2g} g_{Eg}, \quad (40)$$
$$\frac{dg_{Eg}}{d\ell} = -\left(g_{A1g} - g_{Eg}\right)^2 - \left(g_{A2g} - g_{Eg}\right)^2 - 10 g_{Eg}^2. \quad (41)$$

Note that even if not present initially, g_{E_g} is generated first since it has a term proportional to $g_{A_{1g}}^2$, and since its beta function is negative definite, it becomes more and more negative under RG. The $g_{A_{2g}}$ coupling is generated only after g_{E_g} has been generated.

The couplings typically run away along rays (see OV and Kun Yang, PRB 81, 04140(R) (2010)). We can see that by following argument: consider the ratio of the first two flow equations and the third one

$$\frac{dg_{A_{1g}}}{dg_{E_g}} = f_1 \left(\frac{g_{A_{1g}}}{g_{E_g}}, \frac{g_{A_{2g}}}{g_{E_g}} \right) \quad (42)$$
$$\frac{dg_{A_{1g}}}{dg_{E_g}} = f_2 \left(\frac{g_{A_{1g}}}{g_{E_g}}, \frac{g_{A_{2g}}}{g_{E_g}} \right), \quad (43)$$

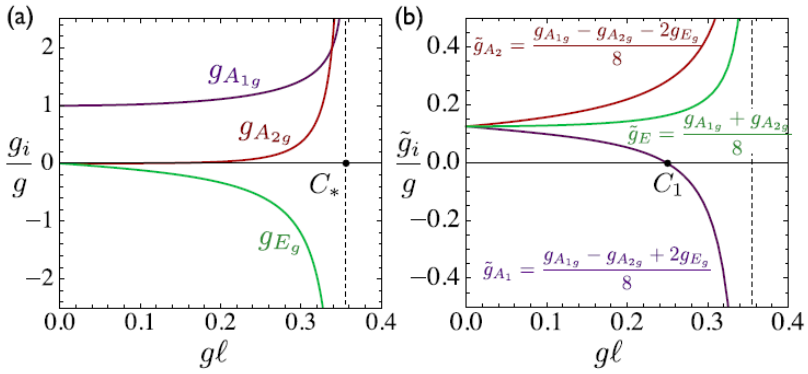

Figure 3: (a) Flow of the interaction couplings when initially $g_{A_{1g}}(0) > 0$, while all other couplings vanish initially. Under these conditions, only two other couplings get generated under RG: $g_{A_{2g}}(0)$ and $g_{E_g}(0)$. (b) Same as in panel (a), but the quartic terms in ψ are rewritten via a Fierz transformation in terms of Cooper pair-Cooper pair. The resulting couplings are labeled $\tilde{g}$. All nine $\tilde{g}$'s are generated, but their values are independent of the $g, u, \mathbf{K}$ labels. Note that for small initial g, then the attractive interactions are generated in the regime where the weak coupling RG is justified.(From OV, J. Murray and V. Cvetkovic PRL 112, 147002 (2014).)

where f_1 and f_2 are readily determined. These equations are invariant under simultaneous rescaling of all couplings by a constant. Therefore,

$$g_{E_g} \frac{d\frac{g_{A_{1g}}}{g_{E_g}}}{g_{E_g}} = -\frac{g_{A_{1g}}}{g_{E_g}} + f_1\left(\frac{g_{A_{1g}}}{g_{E_g}}, \frac{g_{A_{2g}}}{g_{E_g}}\right) \tag{44}$$

$$g_{E_g} \frac{d\frac{g_{A_{2g}}}{g_{E_g}}}{g_{E_g}} = -\frac{g_{A_{2g}}}{g_{E_g}} + f_2\left(\frac{g_{A_{1g}}}{g_{E_g}}, \frac{g_{A_{2g}}}{g_{E_g}}\right). \tag{45}$$

Note that the right hand side is a function of the coupling constant ratios only, and can be thought of as a beta function for the ratios. Zeros of the right hand side determines the fixed rays along which the couplings run away, moreover, linear stability analysis determines which of the rays are stable.

For the special problem with only $g_{A_{1g}}$, $g_{A_{2g}}$, and g_{E_g}, such analysis gives two stable rays:

$$\frac{g_{A_{1g}}}{g_{E_g}} \to 0, \quad \frac{g_{A_{2g}}}{g_{E_g}} \to -0.525$$

and

$$\frac{g_{A_{1g}}}{g_{E_g}} \to 0, \quad \frac{g_{A_{2g}}}{g_{E_g}} \to 13.98.$$

For the initial conditions $g_{A_{1g}} > 0$, $g_{A_{2g}} = g_{E_g} = 0$, the first ray is approached.

An important insight into the problem can be gained by *exactly* recasting the interaction term in the action as a pairing interaction (for details see OV, J. Murray and V. Cvetkovic PRL 112, 147002 (2014).)

$$S^{int}_{eff} = \int_0^\beta d\tau \int d^2\mathbf{r}\mathcal{L}_{\text{int}}$$

and

$$\mathcal{L}_{\text{int}} = \frac{1}{2}\sum_{j=1}^{10} \tilde{g}_j \mathrm{S}_j^\dagger(\mathbf{r},\tau)\mathrm{S}_j(\mathbf{r},\tau) + \frac{1}{2}\sum_{j=11}^{16} \tilde{g}_j \vec{\mathrm{T}}_j^\dagger(\mathbf{r},\tau)\cdot\vec{\mathrm{T}}_j(\mathbf{r},\tau) \tag{46}$$

where the spin singlet and the spin triplet Cooper pair terms are

$$\mathrm{S}_j(\mathbf{r},\tau) = \sum_{\alpha,\beta=\uparrow,\downarrow} \psi^T_\alpha(\mathbf{r},\tau)\Gamma^{(s)}_j (i\sigma_2)_{\alpha\beta}\,\psi_\beta(\mathbf{r},\tau), \tag{47}$$

$$\vec{\mathrm{T}}_j(\mathbf{r},\tau) \;=\; \sum_{\alpha,\beta=\uparrow,\downarrow} \left(\psi^T_\alpha(\mathbf{r},\tau)\Gamma^{(t)}_j \left(i\sigma_2\vec{\sigma}\right)_{\alpha\beta}\psi_\beta(\mathbf{r},\tau)\right). \tag{48}$$

The 9 independent pair interactions, $\tilde{g}_j$, can be written as a linear combination of g_j's using Fierz identities

$$\tilde{g}_{R_p} = \frac{1}{8}\sum_{R'=A1,A2,E} \mathcal{F}_{RR'} \sum_{p'=g,u,\mathbf{K}} \mathcal{F}_{pp'} g_{R'_{p'}} \tag{49}$$

where $\mathcal{F} = \begin{pmatrix} 1 & -1 & 2 \\ 1 & -1 & -2 \\ 1 & 1 & 0 \end{pmatrix}$. In other words,

$$\begin{pmatrix} \tilde{g}_{A1_g} \\ \tilde{g}_{A2_g} \\ \tilde{g}_{E_g} \\ \tilde{g}_{A1_u} \\ \tilde{g}_{A2_u} \\ \tilde{g}_{E_u} \\ \tilde{g}_{A1_\mathbf{K}} \\ \tilde{g}_{A2_\mathbf{K}} \\ \tilde{g}_{E_\mathbf{K}} \end{pmatrix} = \frac{1}{8}\begin{pmatrix} 1 & -1 & 2 & -1 & 1 & -2 & 2 & -2 & 4 \\ 1 & -1 & -2 & -1 & 1 & 2 & 2 & -2 & -4 \\ 1 & 1 & 0 & -1 & -1 & 0 & 2 & 2 & 0 \\ 1 & -1 & 2 & -1 & 1 & -2 & -2 & 2 & -4 \\ 1 & -1 & -2 & -1 & 1 & 2 & -2 & 2 & 4 \\ 1 & 1 & 0 & -1 & -1 & 0 & -2 & -2 & 0 \\ 1 & -1 & 2 & 1 & -1 & 2 & 0 & 0 & 0 \\ 1 & -1 & -2 & 1 & -1 & -2 & 0 & 0 & 0 \\ 1 & 1 & 0 & 1 & 1 & 0 & 0 & 0 & 0 \end{pmatrix} \begin{pmatrix} g_{A1_g} \\ g_{A2_g} \\ g_{E_g} \\ g_{A1_u} \\ g_{A2_u} \\ g_{E_u} \\ g_{A1_\mathbf{K}} \\ g_{A2_\mathbf{K}} \\ g_{E_\mathbf{K}} \end{pmatrix}. \tag{50}$$

For generic repulsive interactions *all* $\tilde{g}_j$'s are initially repulsive and not obviously conducive to Cooper pairing (see e.g. Fig.3b). Nevertheless, under RG attraction is generated: there is a scale ℓ_1 where $\tilde{g}_i(\ell_1) = 0$ for some i's, and continues negative for $\ell_1 < \ell < \ell_*$. An example of this can be seen in the Fig.3b where $g \equiv g_{A1_g}(0) > 0$ otherwise $g_j(0) = 0$.

2.3 Nature of the instability: susceptibility analysis

Because of the scaling form discussed above, $\ell_1 = C_1/g$, and similarly $\ell_* = C_*/g$, where $C_* > C_1 > 0$. At ℓ_1 the couplings therefore attain values $g_i(\ell_1) = g\Phi_i\left(C_1, \{g_j(0)/g\}\right)$. Since $\Phi_i\left(C_1, \{g_j(0)/g\}\right)$ are finite numbers, independent of g, we arrive at an important conclusion that if g is small then so is $g_i(\ell_1)$; attraction is therefore generated in the regime when the flow equations (**??**) are valid.

However, such attractive pair interactions do not lead to superconductivity, unless, as we will see later, finite chemical potential is introduced. As shown in the Fig.3, the growth of the attractive $\tilde{g}$'s is accompanied by the growth of the repulsive $\tilde{g}$'s, disfavoring superconductivity and favoring an excitonic state. In order to demonstrate this, we introduce infinitesimal symmetry breaking source terms into the starting Hamiltonian,

$$H \to H + \sum_{\mathbf{k}} \left(\sum_{j=1}^{16} \delta H^{(j)}_1 + \sum_{j=1}^{10} \Delta^{pp}_j \delta H^{(j)}_{2s} + \sum_{j=11}^{16} \vec{\Delta}^{pp}_j \cdot \delta H^{(j)}_{2t}\right),$$

where

$$\delta H^{(j)}_1 = \psi^\dagger_{\mathbf{k},\alpha}\left(\Delta^{ph}_j \Gamma_j \delta_{\alpha\beta} + \vec{\Delta}^{ph}_j \cdot \Gamma_j \vec{\sigma}_{\alpha\beta}\right)\psi_{\mathbf{k},\beta},$$

and

$$\delta H^{(j)}_{2(s,t)} = \frac{1}{2}\psi^T_{\mathbf{k},\alpha}\Gamma^{(s,t)}_j \left(i\sigma_2\left(1,\vec{\sigma}\right)\right)_{\alpha\beta}\psi_{-\mathbf{k},\beta} + H.c.$$

Using our RG procedure we find

$$\frac{d\ln\Delta^{ph}_i}{d\ell} \;=\; 2 + B^{ph}_{ij} g_j(\ell), \tag{51}$$

$$\frac{d\ln\Delta^{pp}_i}{d\ell} \;=\; 2 + B^{pp}_{ij} g_j(\ell). \tag{52}$$

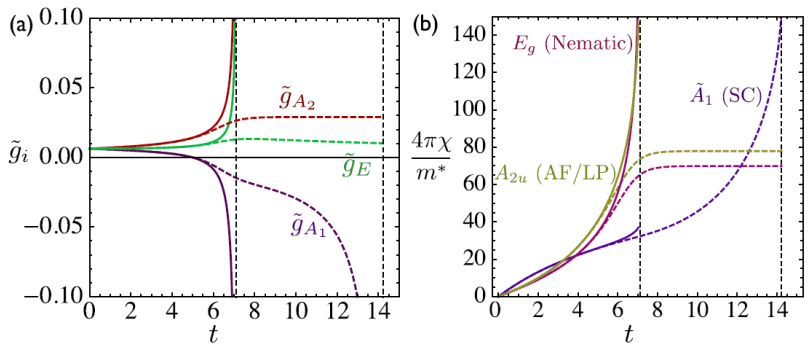

Figure 4: (a) Flow of the interaction couplings when initially $g_{A_{1g}}(0) > 0$, while all other couplings vanish initially. Solid lines are for negligibly small chemical potential leading to nematic. Dashed lines for finite chemical potential satisfying $\frac{\Lambda^2}{2m^*}e^{-2C_*/g} \ll \mu \ll \frac{\Lambda^2}{2m^*}e^{-2C_1/g}$ leading to a superconductor. (b) Susceptibilities: solid line no chemical potential, dashed line finite chemical potential satisfying $\frac{\Lambda^2}{2m^*}e^{-2C_*/g} \ll \mu \ll \frac{\Lambda^2}{2m^*}e^{-2C_1/g}$. The variable t is related to ℓ by $t = \frac{1}{2}\ln\left(\frac{\Lambda^2/2m^*-\mu}{e^{-2\ell}\Lambda^2/2m^*-\mu}\right)$. (From OV, J. Murray and V. Cvetkovic PRL 112, 147002 (2014).)

The coefficients B_{ij} are determined from the diagrams shown in Fig.2d. as well as the dependence of the Helmholtz free energy, δf, on Δ_j's and ℓ:

$$\delta f(\Delta;\ell) = -\frac{m^*}{16\pi}\sum_{j=1}^{32}\int_0^\ell d\ell' e^{-4\ell'}\left[\Delta_j^{ph/pp}(\ell')\right]^2\alpha_j^{ph/pp} \tag{53}$$

This is then used to compute the susceptibility,

$$\chi_{ij}(\ell) = -\frac{\partial^2\delta f}{\partial\Delta_i^*\partial\Delta_j},$$

associated with excitonic or superconducting ordering tendencies. These susceptibilities can be determined analytically along the rays, and therefore also in the asymptotic regime where the rays are approached. (see V. Cvetkovic, R. Throckmorton, and OV, 86, 075467 (2012)).

By analyzing the fixed rays along which the couplings diverge, we see that despite generating the attractive interactions at ℓ_1, the susceptibility in the excitonic channels grows above the superconducting ones (solid lines in Fig.4b). With pure forward scattering, the dominant instability appears to be the charge nematic corresponding to

$$\alpha\psi_\sigma^\dagger 1\sigma_1\psi_\sigma + \beta\psi_\sigma^\dagger\tau_3\sigma_2\psi_\sigma.$$

Were we to start with initial conditions $g_{A_{1g}} = g_{A_{2u}} = 2g_{E_{\mathbf{k}}} > 0$, corresponding to repulsive Hubbard model at the microscopic lattice level, all nine couplings get generated, and the susceptibility analysis identifies the layer antiferromagnetic state

$$\psi_\alpha^\dagger 1\sigma_3\vec{\sigma}_{\alpha\beta}\psi_\beta$$

as the leading instability. (OV PRB 82, 205106 (2010); V. Cvetkovic, R. Throckmorton, and OV, 86, 075467 (2012).)

Were we to start with initial conditions $g_{A_{1g}} = g_{A_{2u}} = 2g_{E_{\mathbf{k}}} < 0$, corresponding to attractive Hubbard model at the microscopic lattice level, all nine couplings get generated as well. The susceptibility analysis identifies the layer polarized state

$$\psi_\sigma^\dagger 1\sigma_3\psi_\sigma$$

and

$$\psi_\alpha^\dagger\tau_1 1 i\sigma^y_{\alpha\beta}\psi^*_\beta + H.c.$$

as the leading instability. Such degeneracy is a consequence of SO(4) symmetry of the Hubbard model. Further range interactions cause splitting of the degeneracy between the charge ordered state and the s-wave superconductor (V. Cvetkovic, R. Throckmorton, and OV, 86, 075467 (2012)).

2.4 Finite chemical potential and superconductivity

Consider the non-interacting problem with a finite value of the chemical potential

$$\mu \sum_n \sum_{\mathbf{k}} \sum_{\sigma=\uparrow,\downarrow} \psi^\dagger_{n,\mathbf{k},\sigma} \psi_{n,\mathbf{k},\sigma}.$$

If we choose to perform the RG procedure using the same prescription as before, then the chemical potential μ grows under the rescaling:

$$\mu_\ell = \mu e^{2\ell}.$$

Free energy calculated using our RG or by simply using the known results for the non-interacting case are identical, as they should be.

When we turn on the interactions, we perform our RG procedure the same way. We would like to think of the chemical potential, clearly a relevant perturbation, analogously to the mass parameter of the bosonic n-vector field model (P. M. Chaikin and T. C. Lubensky, Principles of Condensed Matter Physics (Cambridge University Press, Cambridge, UK, 1995), p. 266.). There is a crucial difference, however, in that Cooper instabilities are not suppressed by finite μ.

It is convenient to write the chemical potential as

$$(\mu + \delta\mu) \sum_n \sum_{\mathbf{k}} \sum_{\sigma=\uparrow,\downarrow} \psi^\dagger_{n,\mathbf{k},\sigma} \psi_{n,\mathbf{k},\sigma},$$

where $\delta\mu$ is the exact value of the chemical potential at half filling. Therefore, at half filing, $\mu = 0$. We can determine the value of $\delta\mu$ exactly using the particle-hole transformation on the Fermi operators (not the Grassman fields) (J. Murray and OV, PRB 89, 205119 (2014)):

$$\psi_{\mathbf{k}\sigma} = \tau_1 \sigma_3 \chi^*_{-\mathbf{k}\sigma} \tag{54}$$

$$\psi^*_{\mathbf{k}\sigma} = \tau_1 \sigma_3 \chi_{-\mathbf{k}\sigma}. \tag{55}$$

The expectation values of the ψ- and χ- particle numbers are related by

$$\sum_{\mathbf{k}} \langle \psi^*_{\mathbf{k}\sigma} \psi_{\mathbf{k}\sigma} \rangle = \sum_{\mathbf{k}} \left(8 - \langle \chi^*_{\mathbf{k}\sigma} \chi_{\mathbf{k}\sigma} \rangle \right). \tag{56}$$

Therefore, if

$$\sum_{\mathbf{k}} \langle \psi^*_{\mathbf{k}\sigma} \psi_{\mathbf{k}\sigma} \rangle = \sum_{\mathbf{k}} \langle \chi^*_{\mathbf{k}\sigma} \chi_{\mathbf{k}\sigma} \rangle,$$

then the system is at half filling: only half of the eight modes per $\mathbf{k}$ are occupied. In order for the expectation values to be equal, they must be described by the same Hamiltonians, with the same chemical potentials. Working out the anti-commutators in the normal ordered Hamiltonian in terms of χ's, we find that the condition to be at half-filling is achieved if

$$\frac{\delta\mu}{\Lambda^2/2m^*} = \sum_{j=1}^{9} c_j g_j = 8 g_{A_{1g}} - \left(g_{A_{1g}} + g_{A_{2g}} + 2 g_{E_g} + g_{A_{1u}} + g_{A_{2u}} + 2 g_{E_u} + 2 g_{A_{1\mathbf{K}}} + 2 g_{A_{2\mathbf{K}}} + 4 g_{E_{\mathbf{K}}} \right) \tag{57}$$

$$\mu = 0. \tag{58}$$

The expression (57) remains valid when the coupling flow, i.e. $\delta\mu \to \delta\mu_\ell$ and $g_j \to g_j(\ell)$. The contribution to the renormalization of the chemical potential comes from the diagram in Fig.2c. Defining dimensionless chemical potential

$$\tilde{\mu} = \frac{\mu}{\Lambda^2/2m^*} = \frac{\mu}{\Omega_\Lambda},$$

at $T=0$ it is

$$\frac{d\left(\tilde{\mu}+\delta\tilde{\mu}\right)}{d\ell}=2(\tilde{\mu}+\delta\tilde{\mu})-2\sum_{j=1}^{9}c_j g_j(\ell)+\ldots \tag{59}$$

where $\ldots$ represent terms which are second and higher order in g. We note that $2\delta\tilde{\mu}-2\sum_{j=1}^{9}c_j g_j(\ell)=0$ and because $d\delta\tilde{\mu}/d\ell\sim dg/d\ell\sim g^2$ the flow of the chemical potential remains valid to the order we are working if

$$\frac{d\tilde{\mu}}{d\ell}=2\tilde{\mu}+\ldots\ \ \Rightarrow\tilde{\mu}_\ell=\frac{\mu}{\Lambda^2/2m^*}e^{2\ell}. \tag{60}$$

The flow equations for the couplings changes due to the presence of the chemical potential term. Schematically,

$$\frac{dg_j}{d\ell}=A_{ijk}(\tilde{\mu}_\ell+\delta\tilde{\mu}_\ell)g_j g_k+\ldots=A_{ijk}(\tilde{\mu}_\ell)g_j g_k+\ldots \tag{61}$$

The Fourier transform of the imaginary time Greens function is

$$\begin{aligned}G_{\mathbf{k}}(i\omega) &= \left((-i\omega+\mu)\,1_4+\frac{k_x^2-k_y^2}{2m^*}1\sigma_1+\frac{k_xk_y}{m^*}\tau_3\sigma_2\right)^{-1}\\ &= \frac{(i\omega-\mu)\,1_4+\frac{k_x^2-k_y^2}{2m^*}1\sigma_1+\frac{k_xk_y}{m^*}\tau_3\sigma_2}{(\omega+i\mu)^2+\left(\frac{\mathbf{k}^2}{2m^*}\right)^2}\end{aligned} \tag{62}$$

where $\omega_n=(2n+1)\pi T$ is the Matsubara frequency. The following pair of identities is useful in deriving the flow equations

$$\begin{aligned}&\int_{\Lambda(1-d\ell)}^{\Lambda}\frac{dkk}{2\pi}\int_0^{2\pi}\frac{d\theta_{\mathbf{k}}}{2\pi}\int_{-\infty}^{\infty}\frac{d\omega}{2\pi}G_{\mathbf{k}}(i\omega)\otimes G_{\mathbf{k}}(i\omega)=\\ &\frac{m^*}{4\pi}d\ell F_0\left(\frac{\mu}{\Lambda^2/2m^*}\right)\left(-1_4\otimes 1_4+\frac{1}{2}\left(1\sigma_1\otimes 1\sigma_1+\tau_3\sigma_2\otimes\tau_3\sigma_2\right)\right)\end{aligned} \tag{63}$$

$$\begin{aligned}&\int_{\Lambda(1-d\ell)}^{\Lambda}\frac{dkk}{2\pi}\int_0^{2\pi}\frac{d\theta_{\mathbf{k}}}{2\pi}\int_{-\infty}^{\infty}\frac{d\omega}{2\pi}G_{\mathbf{k}}(i\omega)\otimes G_{-\mathbf{k}}(-i\omega)=\\ &\frac{m^*}{4\pi}d\ell\left(F_1\left(\frac{\mu}{\Lambda^2/2m^*}\right)1_4\otimes 1_4+\frac{1}{2}F_2\left(\frac{\mu}{\Lambda^2/2m^*}\right)\left(1\sigma_1\otimes 1\sigma_1+\tau_3\sigma_2\otimes\tau_3\sigma_2\right)\right)\end{aligned} \tag{64}$$

where for $x>0$

$$F_0(x) = \frac{1}{2}\mathrm{sign}\,(1+x)+\frac{1}{2}\mathrm{sign}\,(1-x)\,, \tag{65}$$

$$F_1(x) = \frac{1}{2x}\left(\frac{1+2x}{1+x}-\frac{1-2x}{|1-x|}\right), \tag{66}$$

$$F_2(x) = -\frac{1}{2x}\left(\frac{1}{1+x}-\frac{1}{|1-x|}\right). \tag{67}$$

Note that $F_1(x)=F_2(x)$ for $0\le x\le 1$.

The above results lead to the following equations ($N=4$)

$$\frac{dg_{A1g}}{d\ell} = \left(\left(g_{A1g}^2+g_{A2g}^2+2g_{Eg}^2\right)(F_0-F_1)-2g_{A1g}g_{Eg}(F_0+F_2)+2g_{A2g}g_{Eg}(F_2-F_0)\right), \tag{68}$$

$$\begin{aligned}\frac{dg_{A2g}}{d\ell} &= \big(2g_{A1g}g_{A2g}\,(3F_0-F_1)+2g_{A1g}g_{Eg}\,(F_2-F_0)-4(N-1)g_{A2g}^2F_0\\ &\quad -2g_{A2g}g_{Eg}(5F_0+F_2)+2g_{Eg}^2(F_0+F_1)\big)\,,\end{aligned} \tag{69}$$

$$\begin{aligned}\frac{dg_{Eg}}{d\ell} &= \frac{1}{2}\left(-g_{A1g}^2(F_0+F_2)+2g_{A1g}g_{A2g}(F_2-F_0)+4g_{A1g}g_{Eg}(2F_0-F_1)-g_{A2g}^2(F_0+F_2)\right.\\ &\quad \left.+4g_{A2g}g_{Eg}F_1-4g_{Eg}^2[(N+1)F_0+F_2]\right),\end{aligned} \tag{70}$$

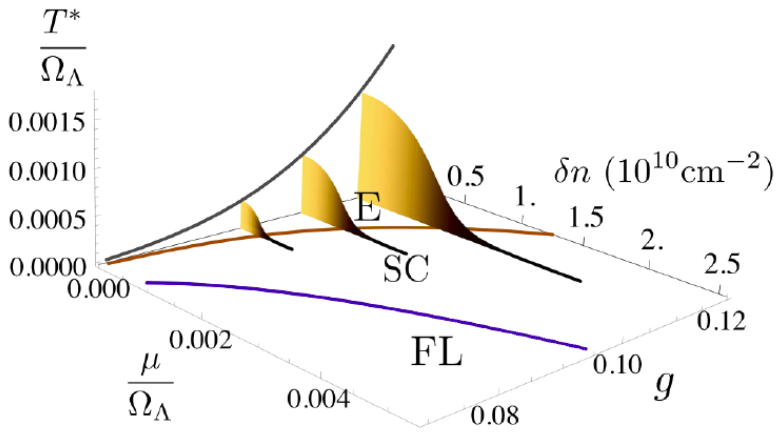

Figure 5: (From OV, J. Murray and V. Cvetkovic PRL 112, 147002 (2014).)

where we omitted the argument of each F_i, which is $\tilde{\mu}_\ell = \frac{\mu}{\Lambda^2/2m^*} e^{2\ell}$. At $\mu = 0$ these equations reduce to those found in Eq.(34). Assuming that only $g_{A1_g}(0) \neq 0$, the value of C_1 can be found rather precisely using series expansion techniques to be $C_1 = 0.248498$. Similarly, the value of $C_* = 0.3553$. The above equations can be rewritten in terms of $\tilde{g}_j$'s using Eq.(50). We find

$$\begin{aligned}
\frac{d\tilde{g}_{A1}}{d\ell} &= -8\tilde{g}_{A1}^2(F_1 + F_2) \\
&- 8\left[-\tilde{g}_{A1}\left((\tilde{g}_{A2} - \tilde{g}_E)N + \tilde{g}_{A2} + 3\tilde{g}_E\right) + \tilde{g}_E((\tilde{g}_{A2} - \tilde{g}_E)N + \tilde{g}_{A2} + 3\tilde{g}_E)\right] F_0 \qquad (71) \\
\frac{d\tilde{g}_{A2}}{d\ell} &= -8\tilde{g}_{A2g}^2(F_1 - F_2) \\
&+ 4\left[\tilde{g}_{A1}^2(N-1) + \tilde{g}_{A2}^2(N+3) + 2\tilde{g}_E\left(\tilde{g}_E - \tilde{g}_{A1} - \tilde{g}_{A2}\right)(N-1)\right] F_0 \qquad (72) \\
\frac{d\tilde{g}_E}{d\ell} &= -8\tilde{g}_E^2 F_1 \\
&- 2\left[N(\tilde{g}_{A1} + \tilde{g}_{A2} - 2\tilde{g}_E)^2 - 3\tilde{g}_{A1}^2 + 2\tilde{g}_{A1}\tilde{g}_{A2} + 12\tilde{g}_{A1}\tilde{g}_E + \tilde{g}_{A2}^2 - 4\tilde{g}_{A2}\tilde{g}_E - 12\tilde{g}_E^2\right] F_0. \qquad (73)
\end{aligned}$$

where, again, we omitted the argument of each F_i, which is $\tilde{\mu}_\ell = \frac{\mu}{\Lambda^2/2m^*} e^{2\ell}$, as well as the specification of the g, u or $\mathbf{K}$ label on $\tilde{g}$, since in this case the result is independent of it. The information contained in Eqs.(68-70) and in Eqs.(71-73) is identical. This can be seen by performing the susceptibility analysis. However, the latter form is more transparent in the regime $\frac{\Lambda^2}{2m^*} e^{-2C_*/g} \ll \mu \ll \frac{\Lambda^2}{2m^*} e^{-2C_1/g}$ due to the manifest decoupling of the equations in the vicinity of the Fermi surface, i.e. when $\ell \approx \sqrt{\frac{\Lambda^2/2m^*}{\mu}}$.

Finite chemical potential introduces a scale ℓ_{FS} at which, were it not for interactions, the chemical potential would reach the cutoff. In other words $\tilde{\mu}_{\ell_{FS}} = 1$. If, in the presence of finite μ, we can guarantee that attraction is generated after $\ell_1 < \ell_{FS}$, but we reach the vicinity of the Fermi surface before the divergence at ℓ_* occurs, i.e. $\ell_{FS} < \ell_*$ then we find superconductivity as the leading instability as is seen in the dashed lines of Fig.(4). Note that the Cooper logarithm appears via the prefactor $1/(1 - \mu_\ell)$ of $\tilde{g}^2$.

In other words, if we wish to guarantee attraction at ℓ_1, we should demand the chemical potential to be negligible at ℓ_1:

$$\tilde{\mu}_{\ell_1} \ll 1.$$

On the other hand, in order to get superconductivity, we wish to reach the Fermi level much before the divergence due to half-filled phase competition occurs at ℓ_*. Therefore, we require

$$\tilde{\mu}_{\ell_*} \gg 1.$$

If both inequalities are to be satisfied, we must have $\frac{\Lambda^2}{2m^*} e^{-2C_*/g} \ll \mu \ll \frac{\Lambda^2}{2m^*} e^{-2C_1/g}$. But, bcause $C_* > C_1$,

we can always reduce g such that the above holds. This guarantees a finite range of chemical potential at which superconductivity emerges.

The scale for the ordering temperature of the superconductor is $\sim e^{-a/g}$, which is manifestly not of the Kohn-Luttinger type which would be $\sim e^{-a'/g^2}$ (see lectures by Steve Kivelson). The resulting phase diagram is shown in Fig.(5)

3 Literature

OV and Kun Yang, PRB 81, 04140(R) (2010).
OV PRB 82, 205106 (2010).
V. Cvetkovic, R. Throckmorton, and OV, 86, 075467 (2012).
R. Throckmorton and OV, PRB 86, 115447 (2012).
OV, J. Murray and V. Cvetkovic PRL 112, 147002 (2014).
J. Murray and OV, PRB 89, 205119 (2014).